Diabetologia (2011) 54:180–189
DOI 10.1007/s00125-010-1944-0

ARTICLE

Deficiency in the extracellular signal-regulated kinase 1 (ERK1) protects leptin-deficient mice from insulin resistance without affecting obesity

J. Jager · V. Corcelle · T. Grémeaux · K. Laurent · A. Waget · G. Pagès · B. Binétruy · Y. Le Marchand-Brustel · R. Burcelin · F. Bost · J. F. Tanti

Received: 19 July 2010 / Accepted: 20 September 2010 / Published online: 15 October 2010

Abstract
Aims/hypothesis Extracellular signal-regulated kinase (ERK) activity is increased in adipose tissue in obesity and type 2 diabetes mellitus and strong evidences suggests that it is implicated in the downregulation of insulin signalling and action in the insulin-resistant state. To determine the role of ERK1 in obesity-associated insulin resistance in vivo, we inactivated *Erk1* (also known as *Mapk3*) in obese leptin-deficient mice (*ob/ob*).

Methods Mice of genotype *ob*/*ob–Erk1*$^{-/-}$ were obtained by crossing *Erk1*$^{-/-}$ mice with *ob*/*ob* mice. Glucose tolerance and insulin sensitivity were studied in 12-week-old mice. Tissue-specific insulin sensitivity, insulin signalling, liver steatosis and adipose tissue inflammation were determined.
Results While *ob*/*ob–Erk1*$^{-/-}$ and *ob*/*ob* mice exhibited comparable body weight and adiposity, *ob*/*ob–Erk1*$^{-/-}$ mice did not develop hyperglycaemia and their glucose tolerance was improved. Hyperinsulinaemic–euglycaemic clamp studies demonstrated an increase in whole-body insulin sensitivity in the *ob*/*ob–Erk1*$^{-/-}$ mice associated with an increase in both insulin-stimulated glucose disposal in skeletal muscles and adipose tissue insulin sensitivity. This occurred in parallel with improved insulin signalling in both tissues. The *ob*/*ob–Erk1*$^{-/-}$ mice were also partially protected against hepatic steatosis with a strong reduction in acetyl-CoA carboxylase level. These metabolic improvements were associated with reduced expression of mRNA encoding inflammatory cytokine and T lymphocyte markers in the adipose tissue.
Conclusions/interpretation Our results demonstrate that the targeting of ERK1 could partially protect obese mice against insulin resistance and liver steatosis by decreasing adipose tissue inflammation and by increasing muscle glucose uptake. Our results indicate that deregulation of the ERK1 pathway could be an important component in obesity-associated metabolic disorders.

Keywords Adipose tissue · Fatty liver · Inflammation · Insulin resistance · Macrophages · Muscles · *ob*/*ob* mice · T lymphocytes

Abbreviations
ACC Acetyl-CoA carboxylase
Akt Thymoma viral proto-oncogene

J. Jager · V. Corcelle · T. Grémeaux · K. Laurent · Y. Le Marchand-Brustel · F. Bost · J. F. Tanti (✉)
INSERM U895, Centre Méditerranéen de Médecine Moléculaire, Team 7 "Cellular and Molecular Physiopathology of Obesity and Diabetes",
Bâtiment Archimed, 151 Route de St Antoine de Ginestière, BP 2 3194, 06204 Nice Cedex 3, France
e-mail: tanti@unice.fr

J. Jager · V. Corcelle · T. Grémeaux · K. Laurent · G. Pagès · Y. Le Marchand-Brustel · F. Bost · J. F. Tanti
Faculty of Medicine, University of Nice Sophia-Antipolis, Nice, France

A. Waget · R. Burcelin
Institut de Médecine Moléculaire de Rangueil, INSERM U858, Toulouse, France

G. Pagès
CNRS UMR 6543, Nice, France

B. Binétruy
INSERM U626, Marseille, France

Y. Le Marchand-Brustel
Centre Hospitalier Universitaire de Nice, Digestive Center, Nice, France

EDL	Extensor digitorum longus
ERK	Extracellular signal-regulated kinase
GIR	Glucose infusion rate
GTT	Glucose tolerance test
MAPK	Mitogen-activated protein kinase
T(h)1	T helper 1
VL	Vastus lateralis

Introduction

The development of obesity in western societies is becoming a major health problem [1]. Obesity is a major risk factor for numerous pathologies, including the development of insulin resistance and type 2 diabetes [2]. Insulin resistance is strongly associated with the development of an inflammatory state in adipose tissue and with ectopic fat accumulation in muscles and liver [3]. Inflammatory cytokines, NEFA and toxic lipid metabolites, such as ceramides and diacylglycerol, activate several signalling pathways that could inhibit insulin signalling [4]. Among these, the pathway involving extracellular signal-regulated kinase (ERK), a mitogen-activated protein kinase (MAPK), is deregulated in obesity and could play a major role in insulin resistance. Indeed, the activity of ERK is abnormally increased in human and rodent adipose tissue in diabetic states [5–7]. Diabetogenic factors, including pro-inflammatory cytokines and lipid metabolites, use the ERK pathway to alter insulin signalling [4, 8]. Further immunological studies have demonstrated that MAPK pathways are involved in the production of inflammatory cytokines by immune cells [9], suggesting a potential role of ERK in the development of inflammation linked to obesity and insulin resistance. Moreover, inflammatory cytokines could increase lipolysis through the ERK pathway, which could be involved in the increase in NEFA responsible, at least in part, for the lipotoxicity [10–13].

ERK1 and ERK2 are the two main proteins of the ERK family, encoded by *Erk1* (also known as *Mapk3*) and *Erk2* (also known as *Mapk1*), respectively. They share 75% overall identity at the amino acid level and are activated by the same stimuli [14]. However, unlike $Erk1^{-/-}$ mice, $Erk2^{-/-}$ mice are not viable, suggesting that these kinases have non-redundant functions [15–17]. We have previously reported that ERK1 rather than ERK2 was involved in adipocyte differentiation and in adipogenesis in vivo [18, 19]. Indeed, $Erk1^{-/-}$ mice have reduced fat content and remain lean when exposed to a high-fat diet. The leanness of the mice on a high-fat diet could be explained, at least in part, by the reduced adipogenesis, but these mice also have an increase in their postprandial metabolic rate that could contribute to the observed phenotype [18]. $Erk1^{-/-}$ mice are also protected against insulin resistance when exposed to a high-fat diet [18]. However, due to the leanness of the mouse, it is not clear whether the invalidation of ERK1 per se is responsible for the improved insulin sensitivity of the $Erk1^{-/-}$ mice fed a high-fat diet.

To address the importance of the ERK1 pathway in the development of obesity-induced insulin resistance, we investigated the impact of *Erk1* deficiency in the context of severe obesity induced by the lack of leptin. Indeed, it is well known that leptin regulates both weight gain and energy expenditure and it could also modulate insulin sensitivity [20]. For this investigation, we intercrossed $Erk1^{-/-}$ mice and leptin-deficient *ob/ob* mice and examined the metabolic responses in the resulting animals. In this setting, despite developing as severe obesity as the *ob*/*ob* controls, *ob*/*ob*–$Erk1^{-/-}$ mice were partially protected against systemic insulin resistance and hepatic steatosis. This metabolic phenotype could be explained by an increase in glucose uptake by muscles and a decrease in adipose tissue inflammation.

Methods

Generation of ob/ob–$Erk1^{+/+}$ and ob/ob–$Erk1^{-/-}$ mice Mice deficient in *Erk1* ($Erk1^{-/-}$ mice) were generated from the C57BL/6J genetic background as previously described by Pages et al. [21]. The $Erk1^{-/-}$ mice were then intercrossed with heterozygote *ob/+* mice to generate double heterozygote mice (*ob/+*–$Erk1^{+/-}$). These mice were then intercrossed to generate *ob/+*–$Erk1^{-/-}$ and *ob/+*–$Erk1^{+/+}$ mice, which subsequently served as parents to lean and obese (*ob/+* and *ob*/*ob*, respectively) animals, either wild type ($Erk1^{+/+}$) or null ($Erk1^{-/-}$) in the *Erk1* locus. Mice were exposed to a 12 h light/dark schedule and had free access to water and standard chow diet. Mice were killed by cervical dislocation and epididymal and subcutaneous fat pads, liver and muscles were removed, freeze-clamped in liquid nitrogen and stored at −80°C until used. The Principles of Laboratory Animal Care (NIH publication no. 85–23, revised 1985; http://grants1.nih.gov/grants/olaw/references/phspol.htm) were followed, as well the European Union guidelines on animal laboratory care (http://ec.europa.eu/environment/chemicals/lab_animals/legislation_en.htm). All procedures were approved by the Animal Care Committee of the Faculty of Medicine of the Nice-Sophia Antipolis University, Nice, France.

Biochemical assays Plasma insulin level was measured using ELISA (Mercodia, Uppsala, Sweden). Quantification of NEFA was performed using a colorimetric diagnostic kit (NEFA-C; Wako Chemicals, Neuss, Germany).

Glucose tolerance test A glucose tolerance test (GTT) was performed on 12 and 18 week old animals after an

overnight fast (~16 h). Glucose (1 g and 0.5 g D-glucose/kg body weight for 12 and 18 week old mice, respectively) was administered by intraperitoneal injection in awake mice. Blood was collected via the tail vein at different time points, and glucose levels were measured using a glucometer (Medisens Optimum XCD; Abbott, Rungis, France).

Hyperinsulinaemic–euglycaemic clamp studies These experiments were performed on 12-week-old animals as described by Burcelin et al. [22, 23]. Under anaesthesia (fluothane), an indwelling catheter was introduced into the femoral vein of the mice, sealed under the back skin, and glued on the top of the skull. The mice were allowed to recover for 4–6 days, and showed normal body weight and feeding behaviour. The clamp studies were conducted with a continuous infusion of insulin (18 mU kg^{-1} min^{-1}) and a variable infusion of glucose (15% [wt/vol.]). To determine the insulin-stimulated glucose utilisation in individual tissues, a rapid intravenous injection of 2-deoxy-D-[^{3}H] glucose (1.85 MBq per mouse; PerkinElmer, Boston, MA, USA) was performed through the femoral vein 60 min before the end of the clamp. Plasma 2-deoxy-D-[^{3}H]glucose disappearance and glucose concentration were determined in 5 μl samples of blood from the tip of the tail vein at 0, 5, 10, 15, 20, 25, 30, 45 and 60 min after injection. Different tissues were dissected for biochemical analysis [24].

For glucose turnover measurement, the level of 2-deoxy-D-[^{3}H]glucose was determined from total blood after deproteinisation by a $Zn(OH)_2$ precipitation as previously described by Perrin et al. [24]. Individual tissue glucose uptake measurement was determined as previously described by Kamohara et al. [25].

Liver triacylglycerol and glycogen content Triacylglycerol extraction was performed on 50 mg of liver homogenised in methanol and chloroform (1:2 [vol./vol.]) over 16 h at 4°C. Then $CaCl_2$ 0.05% (1:5 [vol./vol.]) was added and the samples were centrifuged at 2,000×*g* for 20 min at 4°C. The chloroformic phase was recovered and evaporated and PBS with 5% BSA was added. Triacylglycerol content was determined using a commercial kit (DiaSys, Hozheim, Germany). For histological studies, 10 μm sections were cut from liver samples embedded in paraffin, and were stained with Oil Red O.

To measure glycogen content, 50 mg of liver was homogenised into 1 ml of KOH 0.5 mol/l for 1 h at 60°C. Glycogen was precipitated overnight with 6% Na_2SO_4 (wt/vol.) and 66% ethanol (vol./vol.). The pellet of glycogen was washed three times with 66% ethanol. The glycogen content of the tissue was then measured by an enzymatic method. Briefly, after digestion of the glycogen with 0.25 mg/ml of amyloglucosidase (Sigma, St Louis, MO, USA) for 2 h at 37°C, the glucose concentration of each sample was measured using the Glucose GOD FS kit (DiaSys, Hozheim, Germany).

Insulin-stimulated phosphorylation of Akt and western blot analysis Phosphorylation of thymoma viral proto-oncogene (Akt) (Ser^{473}) was determined in muscle and adipose tissue from *ob*/+, *ob*/*ob* and *ob*/*ob–Erk1*$^{-/-}$ mice after an intraperitoneal injection of insulin (1 U/kg, 10 min). Thereafter, muscles and epididymal fat pads were frozen and stored at −80°C for subsequent analysis.

Muscles or fat pads were solubilised and proteins from lysates were separated by SDS-PAGE and transferred to polyvinylidene difluoride membranes as previously described by our group [8]. The membranes were incubated with the indicated antibody, horseradish-peroxidase-coupled anti-species antibodies were added and chemiluminescence was detected using a Fuji film Las-3000 apparatus (Fujifilm Life Science, FSVT Courbevoie, France). The membranes were subsequently reprobed with the indicated antibody as a loading control. Quantification was performed using MultiGauge software (Fujifilm Life Science).

Antibodies Antibodies against acetyl-CoA carboxylase (ACC), Akt, phospho-Akt (Ser^{473}) and ERK1/2 were purchased from Cell Signaling Technology (Beverly, MA, USA). Horseradish-peroxidase-conjugated secondary antibodies were obtained from Jackson Immunoresearch Laboratories (West Grove, PA, USA).

Real-time RT-PCR Total RNA samples were prepared using the RNeasy total RNA kit (Qiagen, Courteboeuf, France), treated with DNAse (Applied Biosystems, Austin, TX, USA) and used to synthesise cDNAs using Transcriptor First Strand cDNA Synthesis kit (Roche, France). Real-time quantitative PCR was performed with sequence detection systems (ABI PRISM 7500; Applied Biosystems) and SYBR Green dye as previously described. Levels of mRNA were expressed relative to mouse *Rplp0*. The relative amount of mRNA between two groups was determined by using the second derivative maximum method. The results were expressed relative to the mean of the group of controls, which was arbitrarily assigned a value of 1. The primers used (list available on request) were designed using Primer Express software (Applied Biosystems) and synthesised by Eurogentec (Seraing, Belgium).

Statistical analysis All calculations were performed using MINITAB software. Statistical significance between two groups was tested using the Mann–Whitney test. Comparisons among several groups were performed by ANOVA and when the results passed the ANOVA test, Bonferroni's multiple comparison post test was used to calculate the

relevant p values. A p value <0.05 was considered significant. All the data are reported as mean ± SEM.

Results

Erk1 deficiency does not affect the development of obesity in ob/ob mice In the present study, we investigated the consequences of *Erk1* invalidation in obese mice by crossing *Erk1*$^{-/-}$ mice with *ob*/*ob* mice, a model of genetic obesity resulting from leptin deficiency. To determine whether *Erk1* invalidation had consequences for adiposity in mice, the growth curves of *ob*/*ob–Erk1*$^{-/-}$, *ob*/*ob* and *ob*/+ mice were compared. The lack of ERK1 did not modify the weight of the *ob*/*ob* mice (Fig. 1a) and no statistically significant differences were observed in the weight of epididymal and subcutaneous adipose tissues between the two genotypes (Fig. 1b). However, a trend towards a decrease in epididymal adipose tissue and an increase in subcutaneous adipose tissue was noticed in *ob*/*ob–Erk1*$^{-/-}$ compared with *ob*/*ob* mice (Fig. 1b). Hence, the prevention of adiposity development observed in *Erk1*-deficient mice on a high-fat diet [18] was lost in the presence of the *ob*/*ob* background.

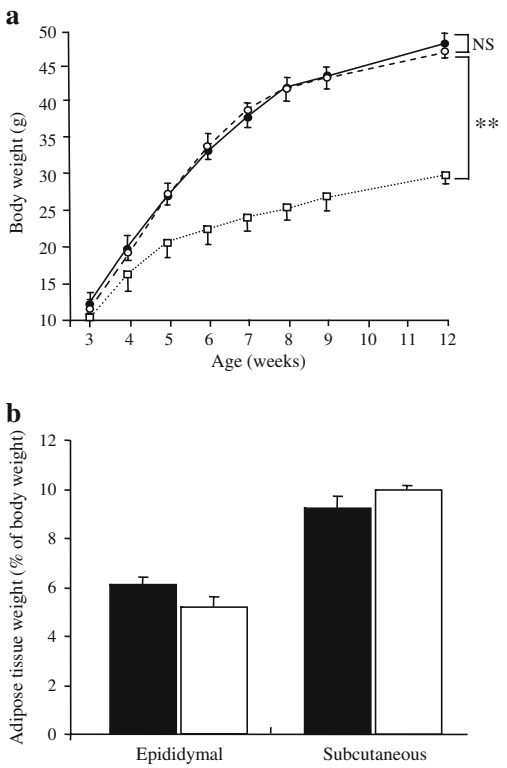

Fig. 1 The *ob*/*ob–Erk1*$^{-/-}$ mice have the same body weight and adiposity as *ob*/*ob* mice. **a** Weight curves of male control *ob*/+, *ob*/*ob* and *ob*/*ob–Erk1*$^{-/-}$ mice (n=8 per genotype). White squares, *ob*/+; black circles, *ob*/*ob*; and white circles, *ob*/*ob–Erk1*$^{-/-}$. **p<0.01 *ob*/+ vs *ob*/*ob* or *ob*/*ob–Ek1*$^{-/-}$ mice. **b** Epididymal and subcutaneous fat pad mass of *ob*/*ob* and *ob*/*ob–Erk1*$^{-/-}$ mice (n=6 per genotype) at 12 weeks of age. Results are expressed as percentage of body weight. Black bars, *ob*/*ob*; white bars, *ob*/*ob–Erk1*$^{-/-}$

ob/ob–Erk1$^{-/-}$ *mice exhibit improved glucose tolerance compared with ob/ob mice* To address the role of ERK1 on whole-body glucose metabolism in obese mice, we next determined blood glucose and serum insulin concentrations in *ob*/+, *ob*/*ob* and *ob*/*ob-Erk1*$^{-/-}$ mice. As expected, fed *ob*/*ob* mice developed hyperglycaemia with severe hyperinsulinaemia compared with lean *ob*/+ mice (Fig. 2a, b). In contrast, *ob*/*ob–Erk1*$^{-/-}$ developed only mild hyperglycaemia but remained hyperinsulinaemic (Fig. 2a, b). Consistent with these results, at 12 weeks of age, obese *ob*/*ob* mice were markedly glucose intolerant compared with control *ob*/+ mice (Fig. 2c). Remarkably, *ob*/*ob–Erk1*$^{-/-}$ mice had an improved glucose tolerance compared with *ob*/*ob* mice (GTT is shown in Fig. 2c and quantification of the response by integrating the AUC is shown in Fig. 2d).

We then tested whether this improved metabolic phenotype was also found in older mice. Analysis of a subgroup of 16–18-week-old mice revealed that older *ob*/*ob–Erk1*$^{-/-}$ retained a lower fed glycaemia (Fig. 2e) and an improved glucose tolerance (GTT in Fig. 2f) without any significant differences in their body weight compared with *ob*/*ob* mice (data not shown).

ob/ob–Erk1$^{-/-}$ *mice exhibit improved whole-body insulin sensitivity and increased insulin action in skeletal muscle* We then performed hyperinsulinaemic–euglycaemic clamp studies in order to quantify whole-body insulin sensitivity and to delineate tissue-specific sites responsible for the improved glucose homeostasis of the *ob*/*ob–Erk1*$^{-/-}$. The steady-state glucose infusion rate (GIR) was increased by 40% in the *ob*/*ob–Erk1*$^{-/-}$ mice compared with *ob*/*ob* mice, demonstrating an improvement in whole-body insulin sensitivity (Fig. 3a). Measurement of glucose utilisation of individual tissues during the clamp revealed that insulin-stimulated glucose disposal rate in vastus lateralis (VL) and the extensor digitorum longus (EDL) skeletal muscles from *ob*/*ob–ERK1*$^{-/-}$ mice was increased by nearly twofold compared with *ob*/*ob* mice (Fig. 3b). As insulin-induced Akt activation is critical for glucose transport, we next investigated the activation of this kinase in EDL muscles following intra-peritoneal insulin injection. Consistent with the increased glucose transport, Akt phosphorylation was higher in insulin-stimulated EDL muscles from *ob*/*ob–Erk1*$^{-/-}$ mice compared with *ob*/*ob* mice (Fig. 3c). However, the level of phosphorylation remained lower than the level observed in control mice (Fig. 3c).

Decreased steatosis in livers of ob/ob–Erk1$^{-/-}$ *mice* Insulin resistance is associated with the accumulation of the ectopic

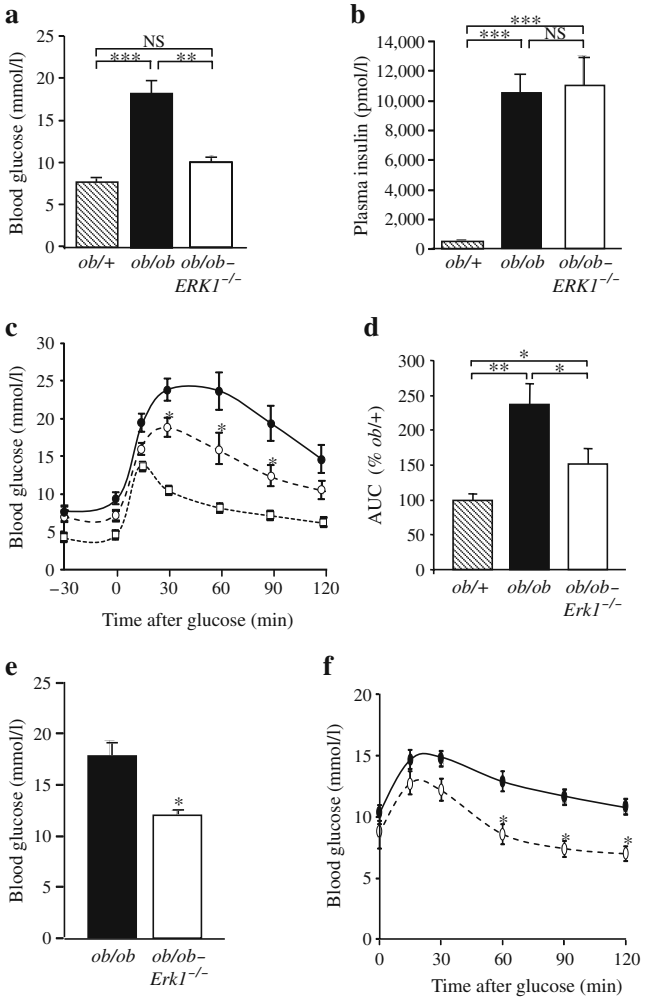

Fig. 2 The *ob/ob-Erk1*$^{-/-}$ mice have reduced fed glycaemia and an improved glucose tolerance compared with *ob/ob* mice. Fed blood glucose concentration **a** and serum insulin concentration **b** of control *ob/+*, *ob/ob* and *ob/ob–Erk1*$^{-/-}$ mice (n=8–10 mice per genotype) at 12 weeks of age; **p<0.01 and ***p<0.001. **c** GTT (1 g D-glucose/kg body weight) was performed with control *ob/+*, *ob/ob* and *ob/ob–Erk1*$^{-/-}$ mice (n=13 per genotype) at 12 weeks of age, after 16 h fasting. White squares, *ob/+*; black circles, *ob/ob*; white circles, *ob/ob–Erk1*$^{-/-}$; *p<0.05. **d** Integrated area under the glucose disposal curves for *ob/ob* and *ob/ob–Erk1*$^{-/-}$ relative to control *ob/+* mice; *p<0.05 and **p<0.01. **e** Fed blood glucose concentration of *ob/ob* and *ob/ob–Erk1*$^{-/-}$ mice (n=4 per genotype) at 16–18 weeks of age; *p<0.05. **f** IGTT (0.5 g D-glucose/kg body weight) was performed with *ob/ob* and *ob/ob–Erk1*$^{-/-}$ mice (n=4 per genotype) at 16–18 weeks of age, after 16 h fasting; *p<0.05. Black circles, *ob/ob*; white circles, *ob/ob–Erk1*$^{-/-}$

fat in liver that participates in the abnormal regulation of glucose homeostasis. We thus investigated whether the improvement in glucose tolerance and whole-body insulin sensitivity of the *ob/ob–Erk1*$^{-/-}$ mice was associated with reduced liver fat content.

Despite the presence of a similar degree of obesity, the liver mass (Fig. 4a) and hepatic triacylglycerol (Fig. 4b) content were reduced by 20% and 35% respectively in *ob/ob–Erk1*$^{-/-}$ mice compared with *ob/ob* mice. Histological examination of liver sections revealed a substantial reduction in the size and number of the lipid droplets in the liver of the *ob/ob–Erk1*$^{-/-}$ mice compared with the *ob/ob* mice (Fig. 4c). The decrease in triacylglycerol content could be due to reduced de novo lipogenesis because the protein level of ACC, a rate-limiting enzyme in de novo lipogenesis, was reduced by 40% in the liver of the *ob/ob–Erk1*$^{-/-}$ (Fig. 4d).

We then investigated whether the reduced amount of hepatic triacylglycerol improved insulin action in the liver of the *ob/ob–Erk1*$^{-/-}$ mice. We measured the amount of glycogen in the liver of *ob/ob* and *ob/ob–Erk1*$^{-/-}$ mice at the end of the 3 h clamp study and interpreted the result as an indication of insulin action. The glycogen content was twofold higher in the liver of *ob/ob–Erk1*$^{-/-}$ mice compared with *ob/ob* mice at the end of the clamp study (Fig. 4e), suggesting a better insulin response.

Decreased obesity-associated inflammation of adipose tissue of the ob/ob–Erk1$^{-/-}$ *mice* Inflammation of adipose tissue as well as an increase in fatty acid release by the tissue has been causally linked to the development of hepatic steatosis and muscle insulin resistance. We thus

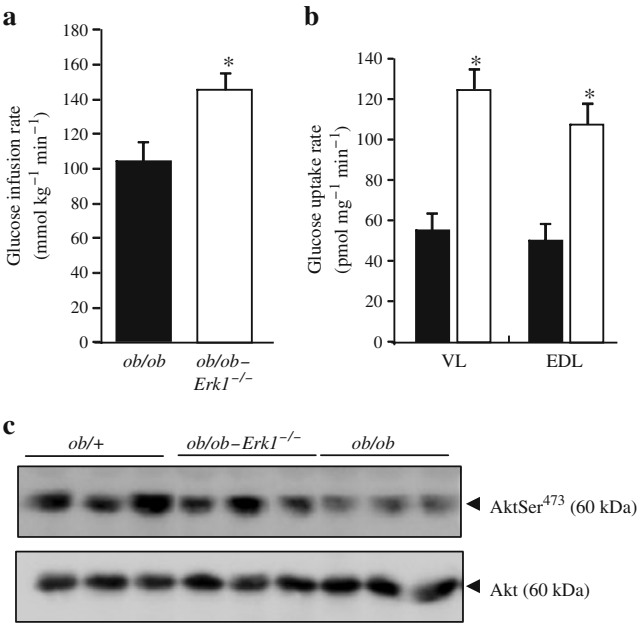

Fig. 3 The *ob/ob–Erk1*$^{-/-}$ mice have improved whole-body insulin sensitivity and an increased glucose utilisation in skeletal muscles. **a** Steady-state GIR during the hyperinsulinaemic–euglycaemic clamp performed with *ob/ob* and *ob/ob–Erk1*$^{-/-}$ mice (n=7–11 per genotype) at 12 weeks of age after 5 h fasting. **b** Glucose uptake rate in VL and EDL muscles during the clamp studies under steady state conditions (n=5–7 per genotype). **c** Representative western blot analysis of the phosphorylation of Akt on Ser^{473} (upper blot) and of total Akt (lower blot) in EDL muscles of *ob/+*, *ob/ob–Erk1*$^{-/-}$ and *ob/ob* mice injected with insulin (1 U/kg, i. p.) for 10 min. *p<0.05. Black bars, *ob/ob*; white bars, *ob/ob–Erk1*$^{-/-}$

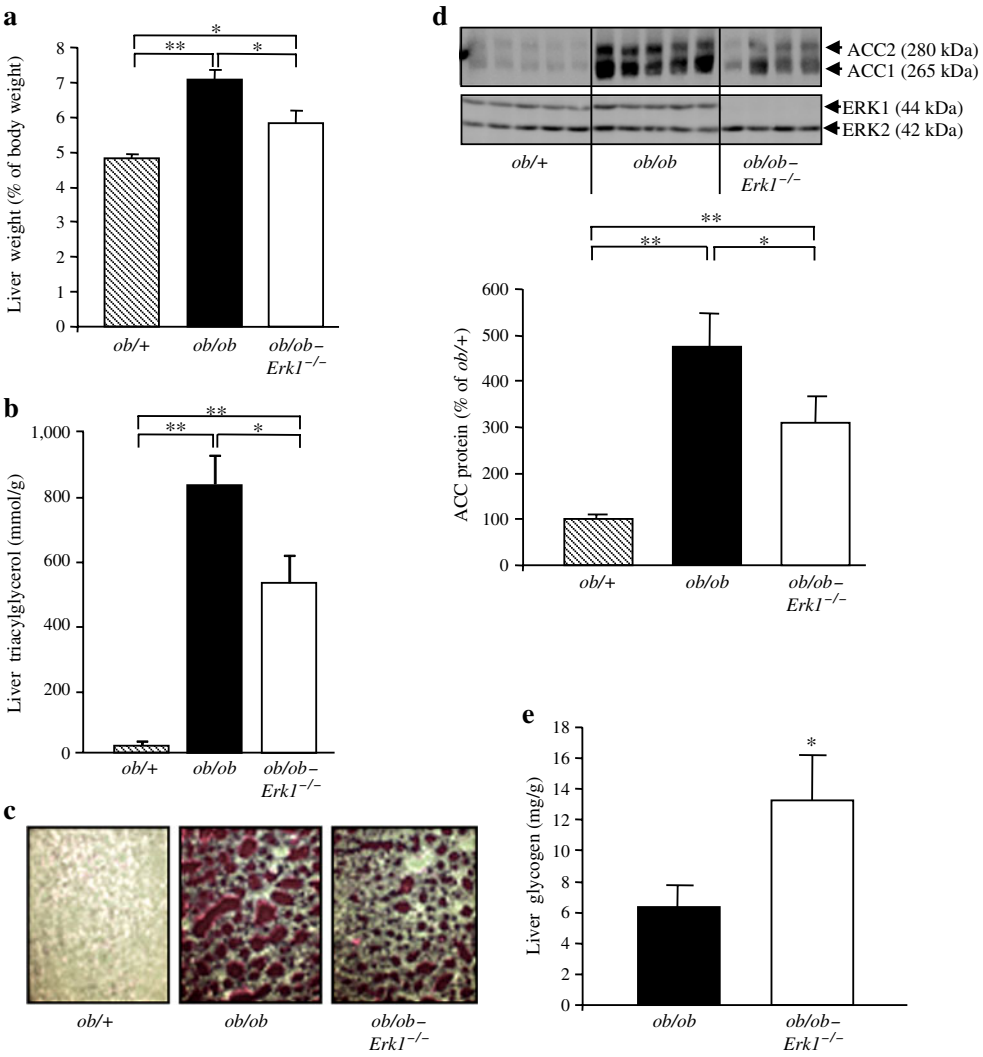

Fig. 4 Reduced hepatic steatosis in the livers of *ob*/*ob*–*Erk1*$^{-/-}$ mice. **a** Liver weights of *ob*/+, *ob*/*ob* and *ob*/*ob*–*Erk1*$^{-/-}$ mice (n=6 per genotype) at 12 weeks of age. Results are expressed as percentage of body weight. **b** Total liver triacylglycerol content was determined for *ob*/+, *ob*/*ob* and *ob*/*ob*–*Erk1*$^{-/-}$ mice (n=7) at 12 weeks of age. **c** Oil red O staining of liver sections of *ob*/+, *ob*/*ob* and *ob*/*ob*–*Erk1*$^{-/-}$ fed mice at 12 weeks of age. **d** Protein lysates from liver were subjected to western blotting with antibodies against ACC1 and ACC2 and against total ERK1/2. Representative immunoblots and quantifications are shown. Data are expressed as percentage of ACC1+ACC2 production in the livers of *ob*/+ mice and are the mean ± SEM of 12–15 mice per genotype. **e** Liver glycogen content in *ob*/*ob* and *ob*/*ob*–*Erk1*$^{-/-}$ mice (n=7–10) at the end of the hyperinsulinaemic–euglycaemic clamp. *p<0.05 and **p<0.01

investigated whether the lack of ERK1 improved the function of the adipose tissue of the *ob*/*ob* mice. Compared with *ob*/*ob* mice, the mRNA levels of several inflammatory markers, such as chemokine (C-C motif) ligand 2 (CCL2), serine protease inhibitor 1 (SERPIN-1*)*, IL1β and TNF, were decreased in epididymal adipose tissue of *ob*/*ob*–*Erk1*$^{-/-}$ mice (Fig. 5a). In contrast, *Il6* and *Il10* mRNA levels were not statistically modified (Fig. 5a). We have recently reported that inflammatory cytokines positively regulate the production of the inflammatory MAP3 kinase tumour progression locus 2 (TPL2; also known as mitogen-activated protein kinase kinase kinase 8 [MAP3K8]) and that its level is upregulated in adipose tissue of obese mice and patients [10]. In agreement with reduced inflammatory cytokine level, we observed a decrease in the *Map3k8* mRNA level in adipose tissue of *ob*/*ob*–*Erk1*$^{-/-}$ mice (Fig. 5a). The expression of *Emr1* (previously known as *F4/80*), which encodes the constitutive macrophage marker EGF-like module containing mucin-like, hormone receptor like sequence 1, was not statistically modified, suggesting that the number of macrophages infiltrating the tissue was not markedly modified by *Erk1* invalidation (Fig. 5a).

As not only macrophages but also T lymphocytes contribute to the development of inflammation in the obese adipose tissue [26], we assessed the mRNA expression of different markers of T lymphocyte populations. The expression of the *Cd3e* mRNA, which codes for the T lymphocyte marker CD3, was reduced suggesting a decrease in T lymphocyte infiltration in the adipose tissue of *ob*/*ob*–*Erk1*$^{-/-}$ mice (Fig. 5b). Recent studies demonstrated that $CD8^+$ and $CD4^+$ T helper 1 (T[h]1) cells dominate in adipose tissue of obese mice [27, 28]. Interestingly, we observed a decrease in *Cd4*, *Ifng* (coding IFNγ a T_H1 cytokine) and *Tbx21* (coding for T-box 21, a marker of T[h]1 cells) mRNA levels in the adipose tissue of *ob*/*ob*–*Erk1*$^{-/-}$ mice. The mRNA expression of *Cd8* was also decreased, but this reduction was not statistically significant (Fig. 5b).

We then studied whether this change in the inflammatory profile of adipose tissue of *ob*/*ob*–*Erk1*$^{-/-}$ was associated

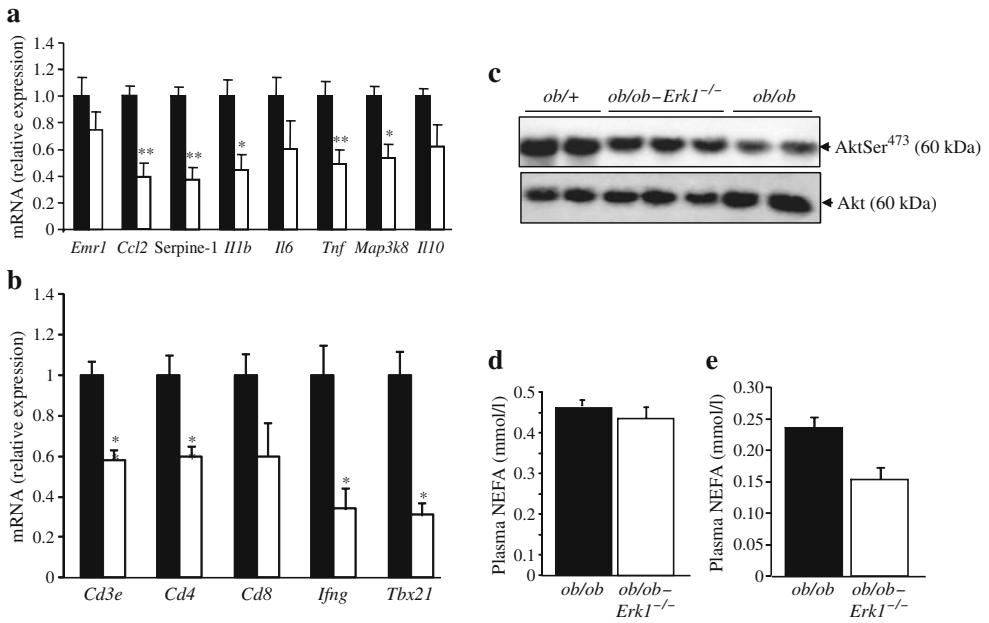

Fig. 5 The *ob*/*ob*–*Erk1*$^{-/-}$ mice have a reduced inflammatory profile in epididymal adipose tissue and an improvement in adipose tissue insulin sensitivity. Relative expression of genes encoding proteins involved in inflammation **a** or T lymphocyte markers **b** in epididymal fat pads from *ob*/*ob* and *ob*/*ob*–*Erk1*$^{-/-}$ mice (n=5–6 per genotype). **c** Representative western blot analysis of the phosphorylation of Akt on Ser^{473} and total Akt in epididymal fat pads of *ob*/+, *ob*/*ob*–*Erk1*$^{-/-}$ and *ob*/*ob* mice injected with insulin (1 U/kg, i.p.) for 10 min. **d**, **e** Adipose tissue insulin sensitivity was assessed by measuring the decrease in plasma NEFA concentration during the clamp study. Results show the circulating NEFA concentration in *ob*/*ob* and *ob*/*ob*–*Erk1*$^{-/-}$ mice (n=6–8 per genotype at 12 weeks of age) following a 6 h fasting period (**d**) and at the end of the hyperinsulinaemic–euglycaemic clamp **e**. *p<0.05 and **p<0.01. Black bars, *ob*/*ob* mice; white bars, *ob*/*ob*–*Erk1*$^{-/-}$ mice

with an improvement in insulin signalling and metabolic action. The Akt phosphorylation was higher in insulin-stimulated adipose tissue from *ob*/*ob-Erk1*$^{-/-}$ mice compared with *ob*/*ob* mice (Fig. 5c). However, the level of phosphorylation remained lower than the level observed in control mice (Fig. 5c). The effect of insulin in adipose tissue was assessed by measuring circulating NEFA levels at the end of the clamp following a 6 h fasting period. After this fasting period, the plasma NEFA levels were not significantly different between *ob*/*ob*–*Erk1*$^{-/-}$ and *ob*/*ob* mice (Fig. 5d). Importantly, after insulin infusion for 3 h, plasma NEFA levels were significantly lower in *ob*/*ob*–*Erk1*$^{-/-}$ mice compared with *ob*/*ob* mice (Fig. 5e), suggesting an amelioration of the anti-lipolytic effect of insulin in adipose tissue.

Discussion

In this study, we demonstrate that although *ob*/*ob* mice lacking ERK1 develop severe obesity, they are partially protected against insulin resistance. The improved glucose homeostasis observed in the *ob*/*ob*–*Erk1*$^{-/-}$ mice is associated with increased glucose transport in muscles, reduced liver fat content and a better ability of insulin to suppress NEFA release by adipose tissue. These metabolic improvements were linked to reduced production of inflammatory cytokines and T lymphocyte markers in the adipose tissue.

Our finding that invalidation of *Erk1* in the C57Bl6/J *ob*/*ob* mice did not prevent the development of obesity differs from the observation made of lean mice on a C57Bl6/J background. Indeed, deletion of *Erk1* in lean mice protected them against high-fat-diet-induced obesity [18]. This protection is due to a relative impairment in adipogenesis and to an increase in postprandial energy expenditure [18]. Leptin is known to regulate postprandial thermogenesis [29]. Hence, the lack of leptin in the *ob*/*ob*–*Erk1*$^{-/-}$ mice could prevent the increase in thermogenesis observed in the high-fat-feeding model and favour the development of fat mass. Alternatively, it is possible that the relative impairment in adipogenesis that we observed in high fat fed *Erk1*$^{-/-}$ mice was dependent on intact leptin signalling.

Importantly, we found that at 12 weeks of age, *ob*/*ob*–*Erk1*$^{-/-}$ mice were partially protected against insulin resistance despite massive obesity, demonstrating that *Erk1* deficiency can influence insulin resistance independently of an effect on the development of obesity. To exclude the possibility that *ob*/*ob*–*Erk1*$^{-/-}$ mice may only have delayed onset of obesity-associated metabolic diseases, we studied a small group of older mice. We found that the

improvement in fed glycaemia and glucose tolerance was retained. However, a deeper investigation with more mice is necessary to answer this question conclusively.

The improvement in insulin sensitivity is associated with a decrease in the expression of genes encoding inflammatory markers in epididymal adipose tissue. Adipose tissue macrophages have been identified as the primary source of inflammatory cytokine production in adipose tissue [30] but it is unlikely that the reduced production of inflammatory markers is due to a decrease in macrophage content in the adipose tissue of *ob*/*ob–Erk1*$^{-/-}$ mice. Indeed, we did not find any significant modification in the expression of the macrophage marker *Emr1* mRNA between *ob*/*ob* and *ob*/*ob–Erk1*$^{-/-}$ mice. Adipose tissue macrophages consist of, at the minimum, classically activated M1 macrophages and alternatively activated M2 macrophages [31–33]. We found that the mRNA levels of several M1 inflammatory genes were decreased in epididymal adipose tissue while the expression of genes encoding inflammation-suppressive factors such as IL-10 was not modified. This result suggests that although *Erk1* invalidation did not markedly affect macrophage numbers, it could modify the ratio of M1 to M2 macrophages. It has been reported that steadily increasing T(h)1 and CD8$^+$ cells numbers could be responsible for a shift to M1 macrophages in obese adipose tissue [27, 28]. This is relevant to our studies because we found that the expression of mRNA of markers of T(h)1 and CD8$^+$ cells was reduced in adipose tissue of *ob*/*ob–Erk1*$^{-/-}$ mice. As a consequence, *Ifng* expression was also reduced, and this could have contributed to a reduction in fat inflammation [34, 35]. Another possible explanation could be an impairment in the production of inflammatory cytokines by M1 macrophage that lack ERK1. Indeed, several cellular studies have reported that the production of some cytokines, including TNF-α and plasminogen activator inhibitor type 1 (PAI-1), depends on ERK activity and that ERK1 rather than ERK2 is involved [36–38]. Nevertheless, our study indicates that the protection from obesity-induced insulin resistance appears to be paralleled by reduced adipose tissue inflammation in the *ob*/*ob–Erk1*$^{-/-}$ mice and this finding underlines a role of ERK1 in fat inflammation.

Our study also revealed a greater ability of insulin to suppress circulating NEFA levels in *ob*/*ob–Erk1*$^{-/-}$ mice compared with *ob*/*ob* mice. This result is indicative of improved insulin action in adipose tissue and is consistent with reduced inflammatory cytokine production. Indeed, the production of phosphodiesterase 3B, a main regulator of the anti-lipolytic effect of insulin, is negatively regulated by TNF-α through an ERK pathway [12]. Further, we have recently shown that the inflammatory cytokines increase ERK activity and lipolysis in rodent and human adipocytes through the activation of TPL2 [10]. Here, we showed that the expression of *Map3k8* mRNA was decreased in the adipose tissue of the *ob*/*ob–Erk1*$^{-/-}$ mice. In adipose tissue, the ERK pathway is also involved in the downregulation of insulin signalling through the negative regulation of IRS production [8]. Among the different IRS proteins, IRS-2, through Akt activation, seems to play a major role in the anti-lipolytic effect of insulin [39]. It is therefore possible that invalidation of *Erk1* prevents the downregulation of IRS-2 in adipose tissue. Consistent with this hypothesis, we found improved Akt activation in the adipose tissue of the *ob*/*ob–Erk1*$^{-/-}$ mice following insulin injection.

It is well known that NEFA have a lipotoxic effect in muscles that leads to an alteration in insulin signalling and action [4, 40]. Interestingly, we found that glucose transport was increased in muscles of *ob*/*ob–Erk1*$^{-/-}$ mice compared with *ob*/*ob* mice and there was also a higher level of insulin-induced Akt activation. Thus, reduced NEFA flux in *ob*/*ob–Erk1*$^{-/-}$ mice could protect muscles against insulin resistance, contributing to the improvement in glucose homeostasis in those mice.

We also found that the amount of triacylglycerol in the liver of the *ob*/*ob–Erk1*$^{-/-}$ mice was reduced by 35% and the size and number of lipid droplets were reduced. This effect could be due to several mechanisms. The reduced NEFA flux from adipose tissue could result in lower ectopic fat deposition in the livers of the *ob*/*ob–Erk1*$^{-/-}$ mice. Further, we found a reduced level of ACC that could limit liver fatty acid synthesis and could also increase fatty acid oxidation through reduced malonyl CoA formation [41]. An increase in the level of ACC and expression of other lipogenic genes is found in the livers of several models of obese mice and could result from an increase in endoplasmic reticulum stress [42, 43]. Endoplasmic reticulum stress could thus be reduced in the liver of the *ob*/*ob–Erk1*$^{-/-}$ mice because of the improvement in glucose and lipid homeostasis. Hepatic accumulation of fatty acid derivatives is involved in the alteration of insulin signalling and action [44]. Thus, the decrease in fat liver content suggests that insulin action could be improved in the liver of the *ob*/*ob–Erk1*$^{-/-}$ mice. In agreement with this hypothesis, we found that the glycogen content of the livers of *ob*/*ob–Erk1*$^{-/-}$ mice was increased following insulin stimulation in the hyperinsulinaemic–euglycaemic clamp studies.

Taken together, our results demonstrate that the lack of ERK1 could partially protect obese mice against insulin resistance and liver steatosis by decreasing adipose tissue inflammation and by increasing muscle glucose uptake. These results link ERK1 activity to the development of insulin resistance independently of its effect on obesity and indicate that deregulation of the ERK1 pathway could be an important component in obesity-associated metabolic disorders. However, because the animal model is a global knockout, we cannot totally exclude that our observations

reflect developmental events. Tissue-specific inactivation of *Erk1* is now needed to answer this important question.

Acknowledgements We thank M. Cormont and S. Peraldi-Giorgetti (INSERM U895, Nice, France) for their critical comments and suggestions. This work was supported by the Institut National de la Santé et de la Recherche Médicale (Paris, France), the University of Nice-Sophia Antipolis (Nice, France) and an ALFEDIAM-Abbott (Paris, France) charity grant to J. F. Tanti. This work is part of the project Hepatic and Adipose Tissue and Functions in the Metabolic Syndrome (HEPADIP, see www.hepadip.org/), which is supported by the European Commission (Brussels, Belgium) as an Integrated Project under the 6th Framework Programme (Contract LSHM-CT-2005-018734). J. Jager was supported by the French Ministry of Research and the Bettencourt Schueller Foundation. J. F. Tanti and F. Bost received support from CNRS and V. Corcelle is a recipient of postdoctoral fellowship of the European Commission (HEPADIP Contract LSHM-CT-2005-018734). Y. Le Marchand-Brustel is the recipient of an Interface grant with the Nice University Hospital (Nice, France).

Duality of interest The authors declare that there is no duality of interest associated with this manuscript.

References

1. Zimmet P, Alberti KG, Shaw J (2001) Global and societal implications of the diabetes epidemic. Nature 414:782–787
2. Hauner H (2004) The new concept of adipose tissue function. Physiol Behav 83:653–658
3. Szendroedi J, Roden M (2009) Ectopic lipids and organ function. Curr Opin Lipidol 20:50–56
4. Tanti JF, Jager J (2009) Cellular mechanisms of insulin resistance: role of stress-regulated serine kinases and insulin receptor substrates (IRS) serine phosphorylation. Curr Opin Pharmacol 9:753–762
5. Bouzakri K, Roques M, Gual P et al (2003) Reduced activation of phosphatidylinositol-3 kinase and increased serine 636 phosphorylation of insulin receptor substrate-1 in primary culture of skeletal muscle cells from patients with type 2 diabetes. Diabetes 52:1319–1325
6. Carlson CJ, Koterski S, Sciotti RJ, Poccard GB, Rondinone CM (2003) Enhanced basal activation of mitogen-activated protein kinases in adipocytes from type 2 diabetes: potential role of p38 in the downregulation of GLUT4 expression. Diabetes 52:634–641
7. Bashan N, Dorfman K, Tarnovscki T et al (2007) Mitogen-activated protein kinases, inhibitory-kappaB kinase, and insulin signaling in human omental vs subcutaneous adipose tissue in obesity. Endocrinology 148:2955–2962
8. Jager J, Gremeaux T, Cormont M, Le Marchand-Brustel Y, Tanti JF (2007) Interleukin-1beta-induced insulin resistance in adipocytes through down-regulation of insulin receptor substrate-1 expression. Endocrinology 148:241–251
9. Dong C, Davis RJ, Flavell RA (2002) MAP kinases in the immune response. Annu Rev Immunol 20:55–72
10. Jager J, Gremeaux T, Gonzalez T et al (2010) The Tpl2 kinase is up-regulated in adipose tissue in obesity and may mediate IL-1β and TNF-α effects on ERK activation and lipolysis. Diabetes 59:61–70
11. Souza SC, Palmer HJ, Kang YH et al (2003) TNF-alpha induction of lipolysis is mediated through activation of the extracellular signal related kinase pathway in 3T3-L1 adipocytes. J Cell Biochem 89:1077–1086
12. Zhang HH, Halbleib M, Ahmad F, Manganiello VC, Greenberg AS (2002) Tumor necrosis factor-alpha stimulates lipolysis in differentiated human adipocytes through activation of extracellular signal-related kinase and elevation of intracellular cAMP. Diabetes 51:2929–2935
13. Greenberg AS, Shen WJ, Muliro K et al (2001) Stimulation of lipolysis and hormone-sensitive lipase via the extracellular signal-regulated kinase pathway. J Biol Chem 276:45456–45461
14. Pouyssegur J, Lenormand P (2003) Fidelity and spatio-temporal control in MAP kinase (ERKs) signalling. Eur J Biochem 270:3291–3299
15. Hatano N, Mori Y, Oh-hora M et al (2003) Essential role for ERK2 mitogen-activated protein kinase in placental development. Genes Cells 8:847–856
16. Saba-El-Leil MK, Vella FD, Vernay B et al (2003) An essential function of the mitogen-activated protein kinase Erk2 in mouse trophoblast development. EMBO Rep 4:964–968
17. Yao Y, Li W, Wu J et al (2003) Extracellular signal-regulated kinase 2 is necessary for mesoderm differentiation. Proc Natl Acad Sci USA 100:12759–12764
18. Bost F, Aouadi M, Caron L et al (2005) The extracellular signal-regulated kinase isoform ERK1 is specifically required for in vitro and in vivo adipogenesis. Diabetes 54:402–411
19. Bost F, Aouadi M, Caron L, Binetruy B (2005) The role of MAPKs in adipocyte differentiation and obesity. Biochimie 87:51–56
20. Ahima RS, Flier JS (2000) Leptin. Annu Rev Physiol 62:413–437
21. Pages G, Guerin S, Grall D et al (1999) Defective thymocyte maturation in p44 MAP kinase (Erk 1) knockout mice. Science 286:1374–1377
22. Burcelin R, Dolci W, Thorens B (2000) Portal glucose infusion in the mouse induces hypoglycemia: evidence that the hepatoportal glucose sensor stimulates glucose utilization. Diabetes 49:1635–1642
23. Burcelin R, Crivelli V, Dacosta A, Roy-Tirelli A, Thorens B (2002) Heterogeneous metabolic adaptation of C57BL/6J mice to high-fat diet. Am J Physiol Endocrinol Metab 282:E834–E842
24. Perrin C, Knauf C, Burcelin R (2004) Intracerebroventricular infusion of glucose, insulin, and the adenosine monophosphate-activated kinase activator, 5-aminoimidazole-4-carboxamide-1-beta-D-ribofuranoside, controls muscle glycogen synthesis. Endocrinology 145:4025–4033
25. Kamohara S, Burcelin R, Halaas JL, Friedman JM, Charron MJ (1997) Acute stimulation of glucose metabolism in mice by leptin treatment. Nature 389:374–377
26. Lumeng CN, Maillard I, Saltiel AR (2009) T-ing up inflammation in fat. Nat Med 15:846–847
27. Nishimura S, Manabe I, Nagasaki M et al (2009) $CD8^+$ effector T cells contribute to macrophage recruitment and adipose tissue inflammation in obesity. Nat Med 15:914–920
28. Winer S, Chan Y, Paltser G et al (2009) Normalization of obesity-associated insulin resistance through immunotherapy. Nat Med 15:921–929
29. Hukshorn CJ, Saris WH (2004) Leptin and energy expenditure. Curr Opin Clin Nutr Metab Care 7:629–633
30. Shoelson SE, Herrero L, Naaz A (2007) Obesity, inflammation, and insulin resistance. Gastroenterology 132:2169–2180
31. Lumeng CN, DelProposto JB, Westcott DJ, Saltiel AR (2008) Phenotypic switching of adipose tissue macrophages with obesity is generated by spatiotemporal differences in macrophage subtypes. Diabetes 57:3239–3246
32. Fujisaka S, Usui I, Bukhari A et al (2009) Regulatory mechanisms for adipose tissue M1 and M2 macrophages in diet-induced obese mice. Diabetes 58:2574–2582
33. Shaul ME, Bennett G, Strissel KJ, Greenberg AS, Obin MS (2010) Dynamic, M2-like remodeling phenotypes of $CD11c^+$ adipose tissue macrophages during high fat diet-induced obesity in mice. Diabetes 59:1171–1181

34. Rocha VZ, Folco EJ, Sukhova G et al (2008) Interferon-gamma, a Th1 cytokine, regulates fat inflammation: a role for adaptive immunity in obesity. Circ Res 103:467–476
35. Duffaut C, Zakaroff-Girard A, Bourlier V et al (2009) Interplay between human adipocytes and T lymphocytes in obesity: CCL20 as an adipochemokine and T lymphocytes as lipogenic modulators. Arterioscler Thromb Vasc Biol 29:1608–1614
36. Rousseau S, Papoutsopoulou M, Symons A et al (2008) TPL2-mediated activation of ERK1 and ERK2 regulates the processing of pre-TNF alpha in LPS-stimulated macrophages. J Cell Sci 121:149–154
37. Skinner SJ, Deleault KM, Fecteau R, Brooks SA (2008) Extracellular signal-regulated kinase regulation of tumor necrosis factor-alpha mRNA nucleocytoplasmic transport requires TAP-NxT1 binding and the AU-rich element. J Biol Chem 283:3191–3199
38. Pandey M, Loskutoff DJ, Samad F (2005) Molecular mechanisms of tumor necrosis factor-alpha-mediated plasminogen activator inhibitor-1 expression in adipocytes. FASEB J 19:1317–1319
39. Previs SF, Withers DJ, Ren JM, White MF, Shulman GI (2000) Contrasting effects of IRS-1 vs IRS-2 gene disruption on carbohydrate and lipid metabolism in vivo. J Biol Chem 275:38990–38994
40. Guilherme A, Virbasius JV, Puri V, Czech MP (2008) Adipocyte dysfunctions linking obesity to insulin resistance and type 2 diabetes. Nat Rev Mol Cell Biol 9:367–377
41. Tong L (2005) Acetyl-coenzyme A carboxylase: crucial metabolic enzyme and attractive target for drug discovery. Cell Mol Life Sci 62:1784–1803
42. Kammoun HL, Chabanon H, Hainault I et al (2009) GRP78 expression inhibits insulin and ER stress-induced SREBP-1c activation and reduces hepatic steatosis in mice. J Clin Invest 119:1201–1215
43. Basseri S, Austin RC (2008) ER stress and lipogenesis: a slippery slope toward hepatic steatosis. Dev Cell 15:795–796
44. Postic C, Girard J (2008) Contribution of de novo fatty acid synthesis to hepatic steatosis and insulin resistance: lessons from genetically engineered mice. J Clin Invest 118:829–838